TEMPERATURE CONTROL OF HIGH POWER MICROPROCESSOR

Ass. Proff. Dr. Abbas Alwi Sakhir Al- Jeebori
Al-Qadisiyah University
College of Engineering
doctor_abbas2001@yahoo.com

Ass. Lecturer Mahmoud A .Hassan
Al-Qadisiyah University
College of Engineering
hasaaneng@yahoo.com

ABSTRACT

Active control of the die-level temperature is desirable during production testing of high power microprocessors, so as to ensure accurate performance classification. The analysis in this research demonstrates fundamentals limits of temperature control for typical devices under test conditions. These limits are identified for specified control power to die power ratios. The effects of test sequence deign and device package design on the temperature control limits are also examined. The theory developed can be applied to any thermal control problem where a conductive medium separates the control source from the location where control is desired. As a dimensional example, when the die power density (Q_d *=10 W/cm*^{2}) and frequency of the die power variation (*w =10 HZ*) with (*DT = 4K*) , the required control power density (Q_c *=63 W/cm*^{2}) . This performance is much better than for ideal temperature control where the control magnitude was found to be (*173 W/cm*^{2}) with no change with the convective heat transfer coefficient f t when it varies from *500 W/m*^{2}*.K* to *2000 W/m*^{2}*.K.*

Keyword: Thermal control**,** Microprocessors**,** Temperature control**,** Power density

السيطرة على درجة الحرارة للمعدات الالكترونية ذي القدرة العالية

أ.م.د عباس عليوي الجبوري م.م. محمود عبد حسان

جامعة القادسية\ كلية الهندسة \ قسم الهندسة الميكانيكية

الخلاصة

السيطرة على درجة حرارة مادة المعالج الالكتروني مهمة جدا" خلال عمليات الإنتاج والفحص للتحقق من دقة الأداء. التحليـــل الرياضي في هذا البحث، يستخدم أساسيات انتقال الحرارة لسيطرة على درجة حرارة معدات الكترونية نموذجية تحت الفحص.

كذلك تم دراسة تأثير عمليات التصميم والفحص على حدود السيطرة على درجة حرارة المعالج الالكتروني. أيضا"، تم توضـــيح عملية السيطرة بمثال نموذجي لمعالج الكتروني ذو قدرة $Q_d=100\ W/cm^2$ وتردد $10\ Hz$ حيث وجـــد أن القـــدرة اللازمـــة للسيطرة هي $Q_c=63\ \ W/cm^2$ وهذا الأداء أفضل من نضيره في عمليات السيطرة العادية حيث يحتاج المعالج الألكتروني الى $Q_c=173W/cm^2$ مع تبات معامل انتقال الحرارة بالحمل h_c ولمعدلات من $500\ W/m^2.K$ إلى $2000\ W/m^2.K$.

NOMENCLATURE

$A(x)$: Cross-sectional area of IHS fin, m^2

A_o: Base cross-sectional area of IHS fin, m^2

a_t: Thermal diffusivity, m^2/s

Bi_{ds}: Biot number for die side of IHS, b / kR_t

Bi_{IHS}: Biot number for top side of IHS, $h_c b / k$

b: Integrated heat spreader IHS Thickness, m

c_p: Specific heat at constant pressure, $J/kg.K$

h_c: Average convective heat transfer coefficient, $W/m^2.K$

i: The imaginary number, $\sqrt{-1}$

k: Thermal conductivity, $W/m.K$

L: Fin length, m

L: Unsteady diffusion scale in IHS, $\sqrt{\omega / 2a_t}$, m^{-1}

m: Mass of die per unit area, kg/m^2

Q_d: Die power density, W / m^2

Q_{da}: Corrected die power density, W / m^2

Q_c: Control power density, W / m^2

R_t: Thermal contact resistance, $K.\ m^2/W$

S: Ratio of die time scale to IHS diffusion time scale

T_{air}: Air temperature, K

T_{die} : Die temperature, *K*

T_{ref} : Reference temperature-often take as zero, *K*

T_{BF} : IHS die side temperature, *K*

t : Time, *s*

X : Real part of complex temperature solution, *K*

x : Distance from reference face of integrated heat spreader, *m*

α , β , γ : Phase shift, *rad*

α : Shaped fin geometry factor

λ : Lumped frequency response of die, $1 / mc_p R_t$, s^{-1}

θ : Temperature defect, $(T-T_{air})$, *K*

ω : Frequency of die power variation, *rad/s*

INTRODUCTION

All high-performance electronic devices are subject to a 100% functional test prior to being shipped by the manufacturer (Pfahnl, et al., 1999). High power microprocessor devices are also subject to a classification test to determine the effective operating speed of the device. During this classification test, the goal of control is to keep the temperature of the die at a single set temperature while the device power is varied between 0% to 100% power in a predetermined test sequence. Temperature increases over the specified test temperature decrease the signal propagation speed within the device, and an excessive temperature rise above the test temperature can result in the device being classified in the wrong category (e.g., a l GHz device classified and shipped as a 950 MHz device). The manufacturer normally specifies a die-level test temperature range; a typical test temperature specification is 85^oC - 0^oC/ + 3^oC.

As microprocessor device powers have increased and device sizes have decreased, the power densities in packaged microprocessor devices have approached levels of 50 to 100 W/cm^2 (Tadayon, 2000). With test sequences rapidly varying the device power at these power densities, active temperature control is essential to holding the die temperature within tolerance. Because the tests are being performed on packaged devices, thermal control cannot be applied to the die itself. Instead, control heating and cooling must be applied to some external part of the packaging. This separation of the control point from the die limits the achievable temperature control tolerances for given test sequences and device powers.

An estimate of the required control power is needed in the early design phases of temperature control systems for test equipment, so that the heating and cooling system capabilities can be

specified. For this reason, an analysis of the packaged device by itself, without any consideration of the control system, is very useful in determining the required minimum heating and cooling capacities as well as in determining the effects of varying the test sequence design and package design on the thermal control limits. This research develops such a model.

MATHEMATICAL MODEL

Semiconductor packaging encompasses a wide range of geometries, die architectures, and materials. In this research, we consider the arrangement shown in **Fig. 1**. The device consists of a silicon die mounted on single or multiple interposer/interface layers. An integrated heat spreader (typically plated copper) is mounted on top of the die structure with a very thin layer of a thermal interface material or grease between the die and the heat spreader. The heat spreader area is typically much larger than the die area and provides a bonding surface for an external heat sink in the final device application. We consider situations in which the die's heat generation is essentially uniform over its area, with no large-scale variations.

Our focus is on temperature under test conditions. During testing, the packaged device is held in a test socket which is itself temperature controlled to the desired test temperature. The socket isolated from the test electronics(Pfahnl, et al., 1998).

Work by Viswanath et al.(2000) and Sweetland(2001) has shown that the thermal resistance between the die structure and the interposer layer is typically much higher than the thermal resistance between the die structure and the surface of the integrated heat spreader. For this reason, only the die and integrated heat spreader will be considered in the transient model (the interposer side of the die is considered adiabatic). If the architecture of a particular device allows non-negligible heat transfer to the interposer, the present results will provide a upper bound on the required control power and a conservative basis for design.

Temperature gradients within the die are taken to be small, effectively making the die a lumped object with uniform internal heat generation. At low frequencies, this approximation is easily justified because the thermal resistance of the interface layer is large compared to that of the die, unless the dies are very thick ($> 1500\ \mu m$). For higher frequencies, analysis of the unsteady conduction in the die, with heat generation confined to the face opposite the integrated heat spreader, shows that the die follows lumped response for the frequencies of importance to the die's thermal response.

To starts the transient analysis, only the temperature profile within integrated heat spreader (IHS) will be considered. For mathematical convenience, that problem can be further decomposed into the two parts shown in **Fig. 2.** The first part is for the IHS with an adiabatic back face and a front surface subject to convective cooling and the radiative control power profile (**Fig. 3A**). The second part is for the IHS with an imposed surface flux from the die on one face and convection on the other face (**Fig. 3B**). The two results are then combined using superposition.

IHS Temperature Response to Control Input

The steady periodic transient response to the two cases in **Fig. 3** can be calculated using a complex temperature approach(Carslaw and Jaeger, 1959). Consider an infinite slab with one side adiabatic as shown in **Fig. 3A**. The other face is subject to convective boundary conditions, an average heat transfer coefficient h_c with an air temperature $T_{air}=0$, and a control flux $Q(t)=Q_c\cos(\omega t)$. Using complex analysis methods, it is assumed that the solution to the temperature profi1e in the complex plane takes the form:

$$W = X(x).\tau(t) \tag{1}$$

where $\tau(t) = e^{i\omega t}$ and $i = \sqrt{-1}$. The conduction equation in the integrated heat spreader is

$$\frac{\partial^2 W}{\partial x^2} = \frac{1}{a_t}\frac{\partial W}{\partial t} \tag{2}$$

so with an assumed solution of Eq. (1), this can be written

$$\frac{d^2 X}{dx^2} = \frac{i\omega}{a_t} \tag{3}$$

which has the general solution

$$X(t) = C_1 \exp\left(-\sqrt{\frac{iw}{a_t}}x\right) + C_2 \exp\left(\sqrt{\frac{iw}{a_t}}x\right) \tag{4}$$

The boundary conditions on Eq. (3) are as follows:

$$x = 0 \qquad \frac{dx}{dx} = 0 \tag{5}$$

$$x = b \qquad -k\frac{dX}{dx} + Q_c = h_c X \tag{6}$$

yields

$$X = \frac{Q_c\, e^{bL}(A - Bi)}{kL(A^2 + B^2)}\left[e^{-xL(i+1)} + e^{xL(i+1)}\right] \tag{7}$$

where

$$A = \left\{ \frac{Bi_{IHS}}{bL} \cos(bL)(e^{2bL} + 1) - [\cos(bL) + \sin(bL)] + e^{2bL}[\cos(bL) - \sin(bL)] \right\} \tag{8}$$

$$B = \left\{ \frac{Bi_{IHS}}{bL} \sin(bL)(e^{2bL} - 1) - [\cos(bL) - \sin(bL)] \right.$$

$$\left. + e^{2bL}[\cos(bL) + \sin(bL)] \right\} \qquad (9)$$

To find the solution to the temperature profile in the integrated heat spreader in the real domain, the real part of $Xe^{i\omega t}$ must be taken

$$T(x,t) = Re(Xe^{i\omega t}) = \frac{Q_c\, e^{L(b-x)}}{kL(A^2 + B^2)}[A\cos(\omega t - xL) + B\sin(\omega t - xL)]$$

$$+ \frac{Q_c\, e^{L(b+x)}}{kL(A^2 + B^2)}[A\cos(\omega t + xL) + B\sin(\omega t + xL)] \qquad (10)$$

IHS Temperature Response to Die Input

An identical approach can be used to find the temperature profile of the integrated heat spreader subject to heat input from the die, but with different boundary conditions are as follows:

$$x = 0 \qquad k\frac{dX}{dx} = h_c X \qquad (11)$$

$$x = b \qquad Q_d = k\frac{dX}{dx} \qquad (12)$$

with Eq. (4) for X, the boundary condition at $x=0$ yields:

$$k\sqrt{\frac{i\omega}{a_t}}(C_2 - C_1) = h_c(C_1 + C_2) \qquad (13)$$

This equation can be solved to express the new C_1 in terms of the new C_2:

$$C_1 = C_2\frac{2(kL)^2 - h_c^2 + (2h_c kL)i}{h_c^2 + 2kh_c L + 2(kL)^2} \qquad (14)$$

in which $L = \sqrt{\omega / 2a_t}$ as before. Defining

$$D = h_c^2 + 2kh_c L + 2(kL)^2, \quad E = 2(kL)^2 - h_c^2, \qquad F = 2h_c kL \qquad (15)$$

Eq. (14) can written

$$C_1 = C_2 \frac{(E + Fi)}{D} \tag{16}$$

and the solution for X becomes

$$X = C_2 \left[\frac{E + Fi}{D} exp\left(-\sqrt{\frac{i\omega}{a_t}} x \right) + exp\left(\sqrt{\frac{i\omega}{a_t}} x \right) \right] \tag{17}$$

Substitution of this expression into the boundary condition at $x=b$ produces

$$Q_d = C_2 kL \left[(i+1) e^{bL} e^{bLi} - \frac{e^{-bL}}{D} (E + Fi)(i+1) e^{-bLi} \right] \tag{18}$$

which may be rearranged to

$$\frac{Q_d}{C_2 kL} = e^{bL} [cos(bL) - sin(bL)] - \frac{e^{-bL}}{D} [G\, cos(bL) + N\, sin(bL)]$$

$$+ e^{bL} i [cos(bL) + sin(bL)] - \frac{e^{-bL}}{D} i [-G\, sin(bL) + N\, cos(bL)] \tag{19}$$

where $G = E - F$ and $N = E + F$ (20)

With the following additional defintions

$$P = e^{bL} [cos(bL) - sin(bL)] - \frac{e^{-bL}}{D} [G\, cos(bL) + N\, sin(bL)] \tag{21}$$

$$R = e^{bL} [cos(bL) + sin(bL)] + \frac{e^{-bL}}{D} [G\, sin(bL) - N\, cos(bL)] \tag{22}$$

the solution for the constant C_2 may be written

$$C_2 = \frac{Q_d (P - Ri)}{kL(P^2 + R^2)} \tag{23}$$

The function X is therefore

$$X = \frac{Q_d (P - Ri)}{kL(P^2 + R^2)} \left[\frac{(E + Fi)}{D} e^{-xL(i+1)} + e^{xL(i+1)} \right] \tag{24}$$

The solution for the temperature in the heat spreader is again found by solving for the real part of $Xe^{i\omega t}$. Setting

$$U = \frac{P.E + R.F}{D} \quad \text{and} \quad V = \frac{P.F - E.R}{D} \tag{25}$$

the final expression for the temperature of the heat spreader is

$$T(x,t) = Re(Xe^{i\omega t}) = \frac{Q_d e^{-xL}}{kL(P^2 + R^2)}[U\cos(\omega t - xL) - V\sin(\omega t - xL)]$$

$$+ \frac{Q_d e^{xL}}{kL(P^2 + R^2)}[P\cos(\omega t + xL) + R\sin(\omega t + xL)] \quad (26)$$

Temperature Response of Die

The die normally has small thermal resistance and can be treated as isothermal for the frequencies of interest. Its temperature response is described by

$$m\, c_p \frac{dT_{die}}{dt} = Q_d \cos(\omega t) - \frac{T - T_{BF}}{R_t} \quad (27)$$

where m is the mass of die per unit area and T_{BF} is the die-side surface temperature of the integrated heat spreader. This equation neglects the heat capacity of the thermal interface material between the die and the IHS. For ideal temperature control, where there is no change in die temperature, and taking the desired die temperature be zero a, the equation for the IHS back face temperature becomes:

$$T_{BF} = -Q_d.R_t \cos(\omega t) = Q_d.R_t \cos(\omega t + \pi) \quad (28)$$

Control Profile Calculation with Specified Die Temperature Tolerance

The two previous analyses identify the control profile for the cases where the die temperature is constant(ideal control)or where the temperature of the back face of the IHS is held constant. To reach actual practice, we must go a step further and allow the die temperature to fluctuate within specified tolerance limits for a given die power profile(non-ideal control). We now adapt the previous analyses to obtain the control power profile for a varying die temperature.

In the lights of Eqs.(27) and (28), we may assume that for non-ideal control, the back face temperature of the HIS has the form

$$T_{BF} = M.Q_d.R_t \cos(\omega t + \beta) \quad (29)$$

where the scaling factor M takes on a value between 0 and 1. Upon substituting Eq. (29) into Eq. (27) and integrating, we obtain

$$T_{die} = \frac{Q_d}{mc_p(\lambda^2 + \omega^2)}\{(1 + M\cos\beta)[\lambda\cos(\omega t) + \omega\cos(\omega t)]$$

$$- \sin\beta[\lambda\sin(\omega t) - \omega\cos(\omega t)]\} \qquad (30)$$

where $\lambda \equiv 1/mc_pR_t$ ($1/\lambda$ is the lumped-capacity time constant associated with Eq. (29). Of interest here is the magnitude of the fluctuation of T_{die}. By setting this magnitude equal to the allowed tolerance ΔT of the die temperature, a relationship between the scaling factor *M* and the phase shift β is obtained:

$$M = -\cos\beta \pm \sqrt{\cos^2\beta - 1 + (mc_p\Delta T/2Q_d)^2(\omega^2 + \lambda^2)} \qquad (31)$$

The goal is to minimized *M* for a given die power profile, since a smaller value of *M* leads to a smaller required control power. Eq. (31) can be differentiated with respect to β

$$\frac{dM}{d\beta} = \sin\beta \mp \frac{\cos\beta\sin\beta}{\sqrt{\cos^2\beta - 1 + (mc_p\Delta T/2Q_d)^2(\omega^2 + \lambda^2)}} = 0 \qquad (32)$$

This equation has to two roots: $\beta = 0$ and $\beta = \pi$. For the case $\Delta T = 0$, the solution must be $M = 1$, not $M = -1$, so the correct root is $\beta = \pi$. Hence

$$M = 1 - \frac{mc_p\Delta T}{2Q_d}\sqrt{(\omega^2 + \lambda^2)} = 1 - \frac{\Delta T}{2Q_dR_t}\sqrt{1 + (\omega/\lambda)^2} \qquad (33)$$

which determines the magnitude of the fluctuation of T_{BF}. The die temperature profile is

$$T_{die} = \frac{Q_d(1 - M)}{mc_p(\lambda^2 + \omega^2)}\{\lambda\cos(\omega t) + \omega\cos(\omega t)\} \qquad (34)$$

The heat flux from the die into the heat spreader, Q_{ds}, may be calculated from Eqs. (29) and (34)

$$Q_{ds} = \frac{T_{die} - T_{BF}}{R_t}$$

$$= \left\{\frac{Q_d\lambda(1 - M)}{mc_pR_t(\lambda^2 + \omega^2)} + MQ_d\right\}\cos(\omega t) + \frac{Q_d\omega(1 - M)}{mc_pR_t(\lambda^2 + \omega^2)}\sin(\omega t)$$

$$Q_{ds} = Q_d\sqrt{\frac{\lambda^2 + M^2\omega^2}{\lambda^2 + \omega^2}}.\cos(\omega t + \gamma) \equiv Q_{da}\cos(\omega t + \gamma) \qquad (35)$$

where

$$\gamma = tan^{-1}\left(\frac{\omega\lambda(M-1)}{\lambda^2 + M\omega^2}\right) \tag{36}$$

and the amplitude Q_{da} is defined as shown. The heat flux from the die into the integrated heat spreader is reduced in magnitude and shifted by a phase lag γ. These revised solutions for the magnitude and phase shift of the flux and temperature at the die side of the IHS can now be used the following equation

$$T_{IHS} = \frac{2Q_c e^{bL}}{kL(A^2+B^2)}\{[A\cos\alpha + B\sin\alpha]\cos(\omega t) + [B\cos\alpha - A\sin\alpha]\sin(\omega t)\}$$

$$+\frac{2Q_d e^{-bL}}{kL(P^2+R^2)}\{[U\cos(bL) + V\sin(bL)]\cos(\omega t) + [U\sin(bL) - V\cos(bL)]\sin(\omega t)\}$$

$$+\frac{2Q_d e^{bL}}{kL(P^2+R^2)}\{[P\cos(bL) + R\sin(bL)]\cos(\omega t) - [P\sin(bL) - R\cos(bL)]\sin(\omega t)\} \tag{37}$$

by setting T_{IHS} in Eq. (37) to T_{BF} from Eq. (39) and setting Q_d in Eq. (37) to Q_{da} from Eq. (35). Upon separating the sine and cosine terms, there obtains:

$$\{PS_2.[A\cos\alpha + B\sin\alpha].Q_c + PS_3 e^{-bL}.[U\cos(bL-\gamma) + V\sin(bL-\gamma)]$$

$$+ PS_3 e^{bL}.[P\cos(bL+\gamma) + R\sin(bL+\gamma)\}\cos(\omega t)$$

$$+\{PS_2.[B\cos\alpha - A\sin\alpha].Q_c + PS_3 e^{-bL}.[U\sin(bL-\gamma) - V\cos(bL-\gamma)]$$

$$- PS_3 e^{bL}.[P\sin(bL+\gamma) - R\cos(bL+\gamma)\}\sin(\omega t)$$

$$= -R_t M.Q_d\cos(\omega t) \tag{38}$$

where

$$PS_1 = \frac{Q_d}{kL(P^2+R^2)}\ ,\ PS_2 = \frac{2e^{bL}}{kL(A^2+B^2)},\ PS_1 = \frac{Q_{da}}{kL(P^2+R^2)} \tag{39}$$

Since Eq. (38) must hold for any time *t*, the solution for Q_c and α may be obtained by requiring that coefficients of the sine and cosine terms of Eq. (38) vanished separately.

$$\left\{\frac{2e^{bL}[A\cos\alpha + B\sin\alpha]}{A^2+B^2}\right\}.\frac{Q_c}{Q_d}.\frac{Q_d}{Q_{da}} = -M.\frac{bL}{Bi_{ds}}.\frac{Q_d}{Q_{da}}$$

$$-\left\{\frac{e^{-bL}[U\cos(bL-\gamma) + V\sin(bL-\gamma) + e^{bL}[P\cos(bL+\gamma) + R\sin(bL+\gamma)}{P^2+R^2}\right\} \tag{40}$$

$$\left\{ \frac{2e^{bL}\,[\,B\cos\alpha - A\sin\alpha\,]}{A^2 + B^2} \right\}\cdot\frac{Q_c}{Q_d}\cdot\frac{Q_d}{Q_{da}} =$$

$$-\left\{ \frac{e^{-bL}\,[\,U\sin(bL-\gamma) - V\cos(bL-\gamma) + e^{bL}\,[\,R\cos(bL+\gamma) - P\sin(bL+\gamma)}{P^2 + R^2} \right\} \qquad (41)$$

where $Bi_{ds} \equiv b/(kR_t)$ is a Biot number for the die side of the IHS. The factors Q_d / Q_{da}, M, and γ depend on the additional groups $Q_d R_t / \Delta T$ and ω / λ. The latter parameter can be written as

$$\frac{\lambda}{\omega} = (bL)^2\left(\frac{2a_t mc_p R_t}{b^2}\right) \equiv (bL)^2 S \qquad (42)$$

Lateral Conduction Effects in IHS

The function of the heat spreader is to act as a fin, conducting heat laterally away from the die. For the steady components of die power, the IHS will indeed function as a fin. For higher frequency components, however, the fin effect will be limited to a frequency-dependent thermal penetration length in the IHS near the die. Only the lower frequency components will have a sufficient penetration depth to influence the control response. In this section, we examine the effect of frequency-dependent lateral conduction on the control requirements.

The Biot number, Bi_{IHS}, for a typical heat spreader is very small, even at the highest h_c values considered here (e.g., $Bi_{IHS} = 0.009$ for $h_c = 2000\ W/m^2K$ and $b = 1.8\ mm$), Thus, the thermal response of the parts of the spreader beyond the die can be modelled using the unsteady fin equation

$$\frac{\partial^2\Theta}{\partial x^2} + \frac{1}{A(x)}\frac{dA}{dx}\frac{\partial\Theta}{\partial x} - \frac{hP}{kA(x)}\Theta = \frac{1}{a_t}\frac{\partial\Theta}{\partial t} \qquad (43)$$

where $\Theta = T - T_{air}$, P is the perimeter subject to convection, $A(x)$ is the cross-sectional area.

A square heat spreader with a square die can be broken into four identical quadrants, by symmetry. The cross-sectional area of the heat spreader can now be expressed as , $A(x) = A_o + bx$, where A_o is the area of the fin along the line of contact with the die.

Equation (43) has been studied extensively, and analytical solutions have been reviewed by Aziz and Kraus(1995). In the present case, with variable cross-sectional area and time dependent

boundary conditions, the equation will be solved using discrete methods. The two items of principal interest are the heat flux and the thermal penetration depth that result from a change in base temperature, with the latter corresponding to the temperature of the IHS directly over the die structure.

The base temperature is never uniform across the thickness of the heat spreader because the powers are time dependent. Nevertheless, this temperature varies over a well specified range, and a bounding value can be used to examine the worst case losses into the fin-like parts of the IHS away from the die. The magnitude of the temperature variation in the IHS over the die can be taken from the previously determined IHS temperature profiles, such as **Fig. 4.** The fin may be divided into the N sections shown in the inset in **Fig. 9.** The temperature of a fin section subject to time varying boundary conditions can be written as

$$\boldsymbol{A.T^{i+1} = T^{i} + F} \qquad (44)$$

where $[\boldsymbol{T^{i}}]$ and $[\boldsymbol{T^{i+1}}]$ are arrays of the fin temperature at time step i and $i+1$ respectively. The details of the forcing function $[\boldsymbol{F}]$ and characteristic matrix $[\boldsymbol{A}]$ are standard, and will not be repeated here. The temperature at time step $i+1$ is found by matrix inversion.

We used this approach to determine the temperature profile in the fin as a function of time subject to changing base temperature T_b^i. The fin was broken into *100* segments and the time step ΔT was decreased by factors of two until successive changes in the time step produced results that varied by less than $0.01^{o}C$ at all times.

RESULTS AND DISCUSSION

Temperature Profile for Die and Back-Face of IHS

As a dimensional example when $Q_d = 10\ W/cm^2$ and $\omega = 10\ HZ$ with $\Delta T = 4\ K$, the required control power profile has a phase shift $\alpha = 377.2^{o}$ and a control magnitude of $Q_c = 63.05\ W/cm^2$. This performance is much better than for ideal temperature control where the control magnitude was found to be $173\ W/cm^2$. The resulting temperature profiles for the die and the back face of the IHS are shown in **Fig. 4**

Model Confirmation

In order to provide an independent confirmation of the mathematical solution an implicit finite difference model(Mills, 1995) of the die/heat spreader system was constructed. This approach is not very convenient for determining for the required control input magnitude and phase shift, but it is very useful for checking the analysis.

Figure 5 shows the die temperature as calculated from the finite difference model for a *10 Hz* die power with $Q_d = 10\ W/cm^2$ The control input has $Q_c = 63.05\ W/cm^2$ and $\alpha = 377.2^o$, as predicted by the analysis for a tolerance of $\Delta T = 4\ K$. As can be seen, the finite difference model confirms that the predicted control input does control the die temperature to the desired level.

Limits to Control for a Given Die Power Profile

A knowledge of the required control power profile for a given temperature tolerance in the die can be used to define the control limits for any given system. Specifically, for a given die power frequency and amplitude, if the control power is limited to some finite value then the die temperature can be controlled only to some minimum tolerance. Tighter temperature control is not possible for that level of control power.

over a range of die power frequencies, the control power ratio, Q_c / Q_d, can be found for a given die temperature tolerance, scaled into the die power as $Q_d R_t / \Delta T$. By evaluating the control power ratio over a range of frequencies, we may define a control limit plot for a specified set of die conditions. **Figure 6** shows such control limits over a range of dimensionless frequency, $(bL)^2$. In this graph, $Bi_{IHS} = 0.0055$, $Bi_{ds} = 0.11$, and $S = 0.76$, corresponding to a *200 μm* thick die, a *1.8 mm* thick copper IHS, $R_t = 0.42\ cm^2K/W$, and convective cooling through $h_c = 1200\ W/m^2K$. (Those values are typical of test conditions currently being developed (Sweetland, 2001)).

Figure 6 shows that any desired die flux to temperature tolerance ratio can be obtained with sufficient control power, so no theoretical limit to temperature control exists. On a practical level, however, power ratios over 3 or 4 quickly become impractical due to cooling requirements of the effective steady state heat load - the sum of the DC components of die power and control power.

These results lead to some very important points. The position of the lefthand sides of the curves are defined by the physical configuration of the heat spreader (thickness, conductivity, etc.), whereas the righthand sides are defined by the mass of the die, frequency of the die power profi1e, and thermal interface resistance between the die and the IHS. If the design of the IC device cannot be altered for thermal purposes, as is usually the case, a desired level of temperature control may instead be obtained by designing the circuit test sequence, for example, so that the die power profile always lies to the right side of the figure.

We may also evaluate the effect of design changes to the integrated heat spreader and thermal interface between the die and IHS. Changing the thermal resistance between the die and the IHS can have a profound effect on the control limits at higher power ratios. This is seen in **Fig. 7A** for $Q_d / \Delta T = 5\ W/cm^2K$. The effects of changing the thickness of the integrated heat spreader and the die are shown in **Fig. 7B and Fig. 7C**, respectively. Changing the thickness of the die (and therefore its mass) has the largest impact on the control limits of the device. The increasing the thickness of the IHS also raised the power required for a given level of control. The effect of changing the convective transfer coefficient h_c is negligible, with no change observed when h_c varies from *500 W/m^{2}K* to *2000 W/m^{2}K*.

Lateral Conduction Results

The heat lost by conduction into the IHS away from the die is found by integrating the flux into the base area, , A_o , over a full period of the harmonic power variation. This heat may be viewed as lost control energy. For example, consider a *1 cm^2 die* and that has a *1.8 mm* thick heat spreader measuring *3.4 cm* by *3.4 cm*. The temperature profile in the part of the IHS not above the die is shown in **Fig. 8** for a *I0 Hz* base temperature variation having a peak-to-peak magnitude of *4 K* with h_c*= 1200 W /m^2K*. The cyclic heat loss is *0.36 W* per fin segment, or *1.44 W* for the entire heat spreader. Similar calculations have been done for a range of frequencies and for various h_c(**Fig. 9**).

The results of such analyses can be used in one of two ways to correct the control response for the lateral conduction losses. One approach is simply to add the control losses to the total control power. The second approach is to provide a control heat flux to an area of the heat spreader larger than the die, so as to minimize time-dependent lateral heat loss from the die (in the case of laser heating of the IHS, this amounts to over-illumination of the IHS). The second option is only really possible for higher frequency signals, because at lower frequencies the penetration depth is of the same order of magnitude as the width of the heat spreader. If the penetration depth is defined as the distance from the base of the fin to the point where the temperature fluctuation is less than *0.1 ^oC*, then the penetration depth for the temperature profile shown in **Fig. 8** is 6.1 *mm*. Illuminating the die area covers *1.0 cm^2*, illuminating the die area and a sufficient edge area to prevent lateral conduction effects on the die area requires illumination of *4.9 cm^2*.

Similarly, the penetration depth for a *40 Hz* signal is *3.4 mm* with over-illumination covering *2.8 cm^2*; and at *100 Hz*, the pentration depth is *2.1 mm* with over-illumination covering *2.0 cm^2*. Assuming the radiant intensity is uniform over the entire illuminated area, over-illumination requires *4.9* times more radiant power at *10 Hz, 2.1* times more at *40 Hz* and *2.0* times the power at *100 Hz*.

CONCLUSIONS

1. Time-leading temperature control in a distributed-parameter thermal system has been evaluated in one and two dimensions. A particular focus has been the testing of packaged, high-power, integrated circuits. The analysis identifies the control power required to bound the temperature variation of a system having time-dependent self-heating if control is by time-varying heat conduction to a position distant from the location being controlled.

2. The results may be very useful in the design of active thermal control systems for testing of electronic devices and for understanding the impact of electronic test-sequence designs and packaging design on the practical limits of temperature control. Three areas of operation for thermal control have been identified. At high frequencies, active control is not required because the temperature deviation without control is below the desired tolerance: steady (DC) cooling is all that is needed. At sufficiently low frequencies, thermal control can be obtained using a system's available control power. For intermediate frequencies, either control is not possible at the system's rated control power and desired temperature tolerance, or larger temperature deviations have to be accepted as a result the system's limitation on control power.

3. This analysis can be applied to any situation where the temperature control source is separated from the active region where temperature control is desired, and should have value for systems other than electronics testing equipment.

REFERENCES

Aziz, A., and Kraus., 1995,"Transient heat transfer in extended surfaces", Applied Mechanics Reviews, 48(7): 317-350.

Carslaw H.S. and Jaeger J.C, 1959, "Conduction of Heat in Solids", Oxford University Press, Oxford, 2nd edition.

Mills, A. F., 1995, "Heat and Mass Transfer", Irwin, Chicago.

Pfahnl A.C., Lienhard J.H., and Slocum A.H., 1999 "Thermal management and control in testing packaged integrated circuit devices". In Proc. 34th Intersociety Energy Conversion conf., Vancouver BC, 1999. Paper No. 1999-0T-2722.

Pfahnl, A.C., Lienhard J.H., and Slocum A.H., 1998, "Temperature control of a handier test interface". In Proc. IEEE Intl. Test Conf., pages 114-118, Washington DC.

Sweetland, M.,2001," Design of Thermal Control Systems for Testing of Electronics", Ph.D. thesis, Massachusetts Institute of Technology, June 2001.

Tadayon, P., 2000, "Thermal challenges during microprocessor testing", Intel Technology Journal, Q3.

Viswanath, R., Wakharkar V., Watwe A., and Lebonheur V, 2000, "Thermal performance challenges from silicon to systems". Intel Technology Journal, Q3

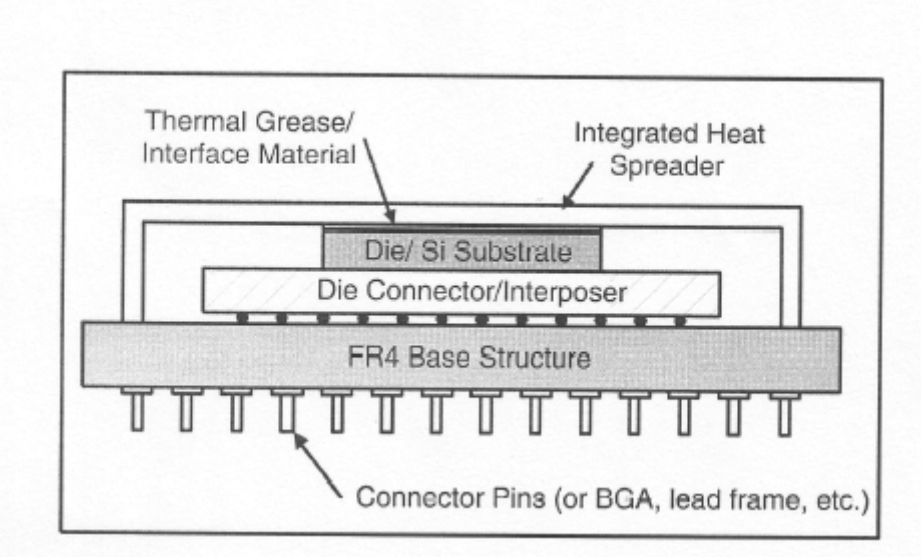

Figure 1: Typical cross-section of a high power microprocessor device.

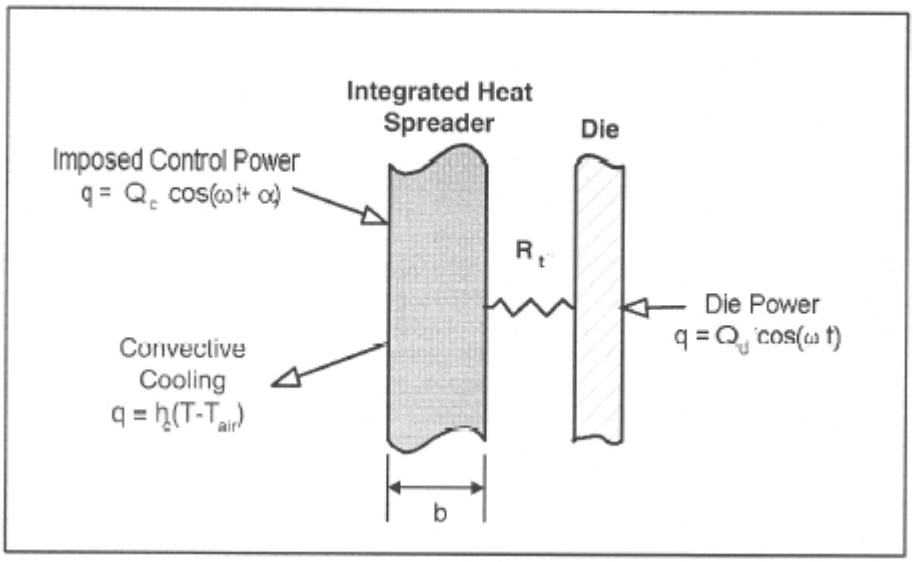

Figure 2: Schematic diagram of simplified device for transient analysis. Q_c is the magnitude of the control input and $\boldsymbol{\alpha}$ is the phase shift of the control input. Q_d is the magnitude of the die power profile.

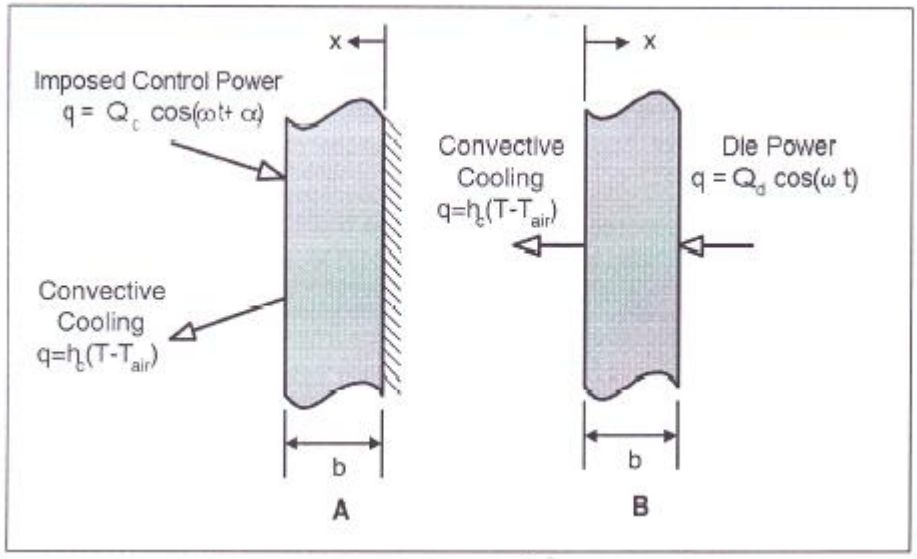

Figure 3: Schematic drawing of decomposition for solution to transient temperature profile in integrated heat spreader.

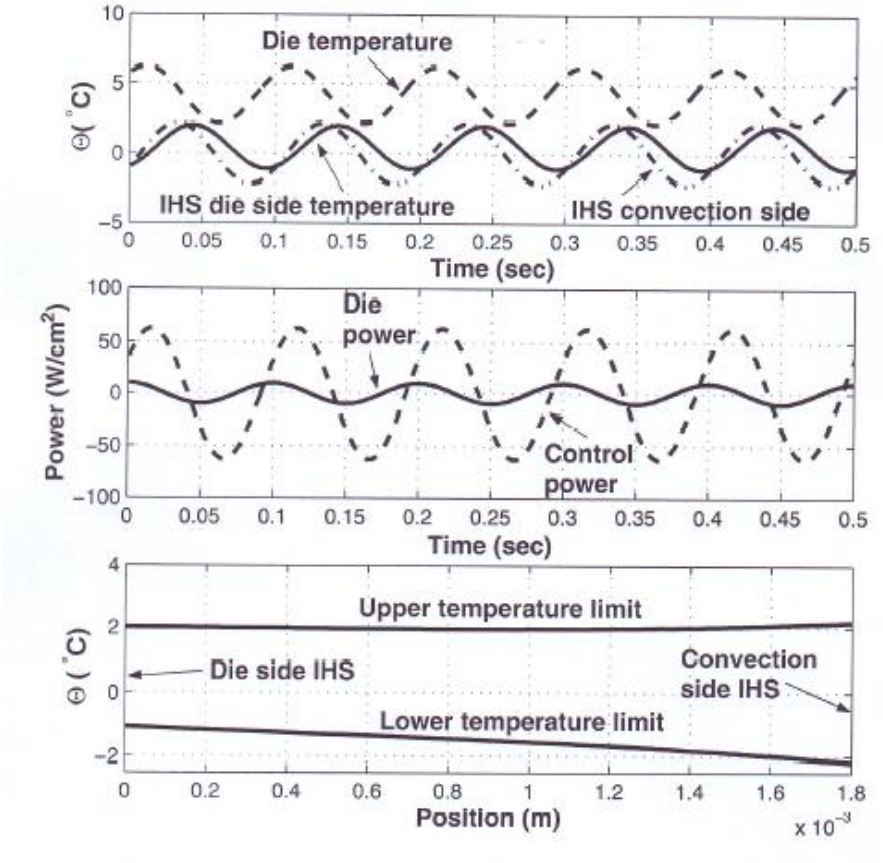

Figure 4: Temperature profile for die and back-face of IHS for $\omega = 10$ Hz, $Q_d = 10$ W / cm^2 and $\Delta T = 4$ K.

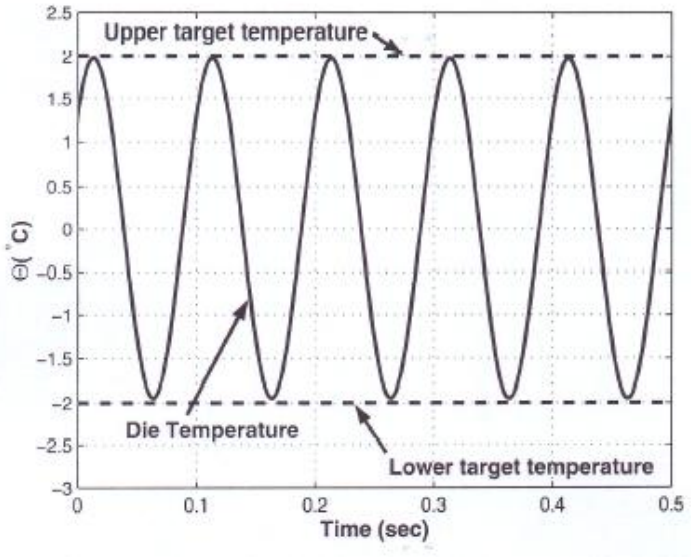

Figure 5: Calculated die temperature using finite difference model to confirm analytic solution for control input. Target $\Delta T = 4$ K with $h_c = 1200$ W/m^{2}K, $R_t = 0.42$ cm^{2}K/W, b=1.8 mm, and $Q_d = 10$ W/cm^2.

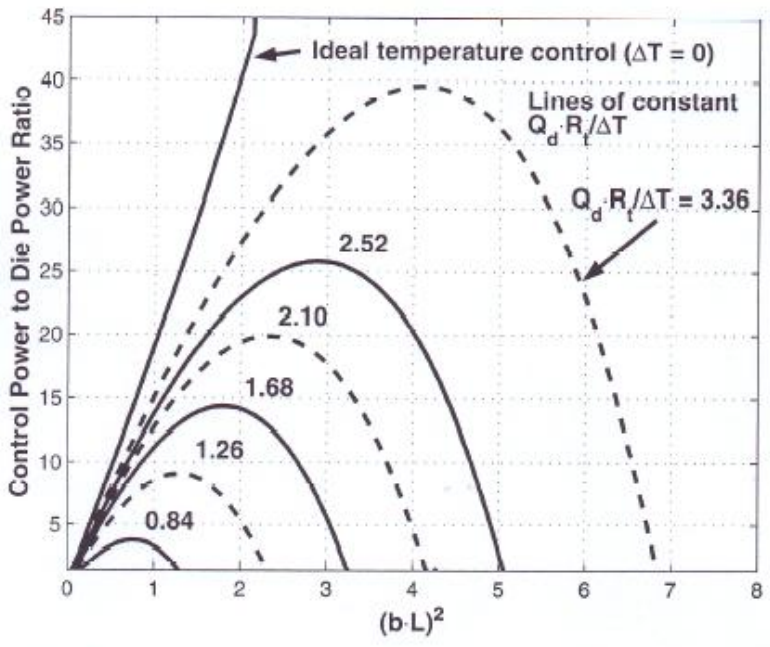

Figure 6: Control power limits for specified die power amplitude, Q_d, and die temperature tolerance, ΔT , as a function of nondimensional die power frequency, $(bL)^2$.

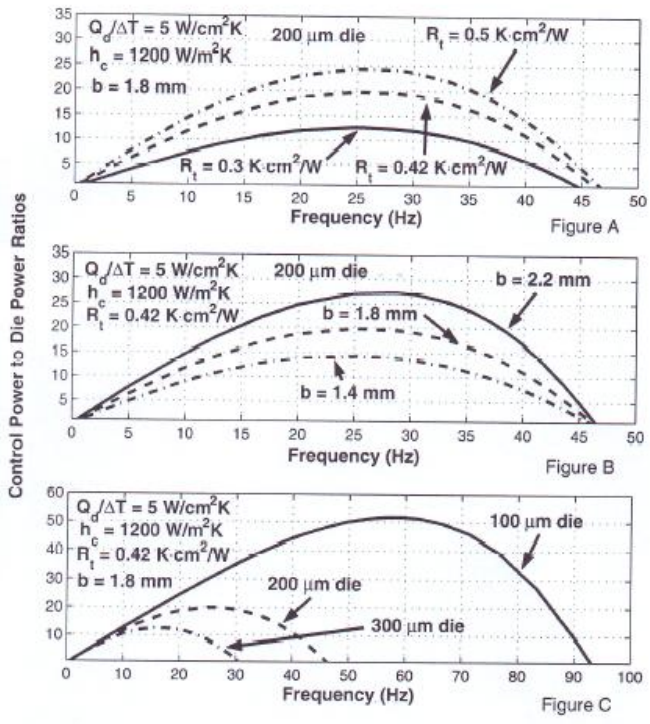

Figure 7: Effect on control power limits of: A- interfacial thermal resistance; B- IHS thickness; and C- die thickness.

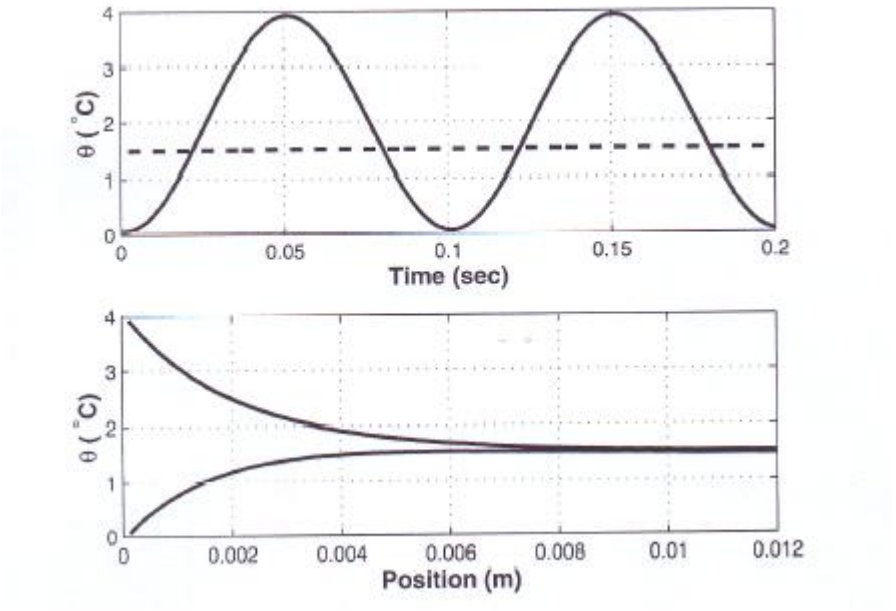

Figure 8: Transient fin temperature profile for *10 Hz* example. Top: temperature variation at base and tip of fin. Bottom: maximum/minimum temperature defect along the length of the fin.

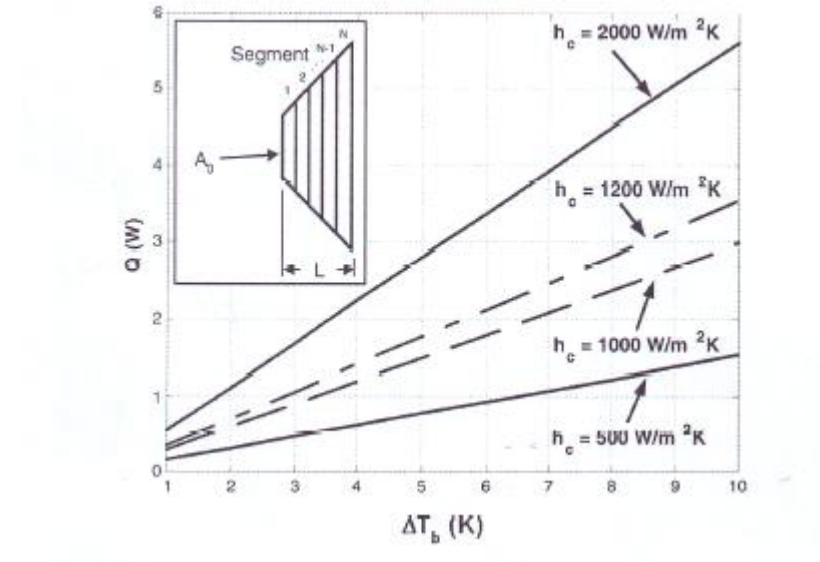

Figure 9: Lateral conduction into IHS for various h_c: Q =cyclic lateral loss into IHS; ΔT_b = temperature fluctuation amplitude of IHS at die edge. Insert shows discretization of IHS for numerical solution.